JOURNAL OF MATERIALS SCIENCE 14 (1979) 1425–1432

Oxygen self-diffusion in a potassium strontium silicate glass using proton activation analysis

B. S. RAWAL*, A. R. COOPER
Division of Metallurgy and Materials Science, Case Western Reserve University, Cleveland, Ohio 44106, USA

Oxygen self-diffusion coefficients were measured in a $20\,K_2O$–$20\,SrO$–$60\,SiO_2$ (wt%) glass above and below the glass transition temperature using the single spectrum proton activation analysis of oxygen-18 using the nuclear reaction $^{18}O(p, \alpha)^{15}N$. The α-particle spectrum recorded during proton irradiation is used to determine the ^{18}O concentration profile. The self-diffusion coefficients, D, determined for the three diffusion times of about 22 h, $3\frac{1}{2}$ and $7\frac{1}{2}$ days were in good agreement within experimental error, except for the two lowest temperatures of the short-time run possibly because of the shallow depths of diffusion and surface exchange. In the temperature range 600 to 1000 K, D values with the relations, above the glass transition temperature

$$D = 7.6 \times 10^{14} \exp(-119\,\text{kcal}/RT)\ \text{cm}^2\,\text{sec}^{-1},$$

and below the glass transition temperature

$$D = 1 \times 10^{-12} \exp(-10\,\text{kcal}/RT)\ \text{cm}^2\,\text{sec}^{-1},$$

were obtained.

1. Introduction

Oxygen is a major constituent of oxide glasses and a knowledge of its self-diffusion coefficients is helpful in understanding the properties of glass. The study of oxygen self-diffusion in $20\,K_2O$–$20\,SrO$–$60\,SiO_2$ (wt%) glass complements the work of Varshneya and Cooper [1–4] who studied the self-diffusion of K and Sr, and multicomponent diffusion in a narrow composition range of this system. The compositions were typical of the commercial compositions of the alkali–alkaline earth silicate systems and the system was chosen for the convenience of electron probe microanalysis.

In recent years, the detection of the stable oxygen isotope ^{18}O by nuclear reactions induced by charged particles such as protons has provided an alternative technique for the study of oxygen diffusion in oxides. In particular, the $^{18}O(p, \alpha)^{15}N$ reaction has been used to probe oxides within a few microns of the surface, the depth being shallow because of the limited penetration of the charged particles in solids. Amsel and co-workers [5–7] have shown that very high sensitivities can be achieved within this shallow depth and were the first to use the "single spectrum" technique [8, 9] to study oxygen diffusion in quartz. The technique was used by Robin *et al.* [10] to its full extent to study the oxygen diffusion in ZnO. The single spectrum technique, the details of which are published elsewhere [10], is briefly described.

2. Single spectrum technique

A monoenergetic proton beam with an incident energy $E_p(0)$ travels through the solid progressively losing energy till at some depth x, $E_p(x) < E_p(0)$, the nuclear reaction is induced. The (p, α) reaction has a positive heat of reaction with $Q = 3.98$ MeV. The energy of the α-particle created at depth x, $E_\alpha(x, x)$, is approximately linearly pro-

*Present address: AVX Ceramics Corporation, Myrtle Beach, South Carolina 29577, USA.

© 1979 Chapman and Hall Ltd. Printed in Great Britain.

portional to $E_p(x)$, and can be calculated using classical kinematics. The α-particle will move through the specimen and lose energy as it travels through the solid. Should its path be in one of the directions to strike one of the detectors, it will be counted according to its energy. At the surface, the α-energy, $E_\alpha(x, 0)$, is a measure of the depth x from which the α-particle was created, and this can be calculated by knowing the stopping powers and the number of α-particles of the target.

One way in which the α-particles are recorded is by passing them through a 12.57 μm thick mylar (polyethylene terephthalate) foil. The mylar foil acts as an absorber for the back-scattered protons, which will otherwise jam the detector due to pile-up. An alternative way is to separate the α-particles from the protons with a magnetic spectrometer, the details of which are given elsewhere [11]. From the sample stopping powers, the reaction cross-section and, if used, the mylar stopping powers, the α-energy at the counter $E_\alpha(x, c)$ can be related to the depth x from which it originated.

However, under experimental conditions, the ideal relationship between E_x (E_x will be used for $E_\alpha(x, 0)$ from now on) and x does not hold. Experimental distortions will spread the one-to-one relationship between a recorded energy and an analysed depth. The alpha particles emitted at depth x will not be recorded at energy E_x but over an energy interval spread around this value. Consequently, the ideal relationship between the number of counts recorded at a given energy and the ^{18}O concentration at the corresponding depth will not be retained.

If mylar foil is used, the primary spreading is caused by α-particles straggling through the mylar and the resolution of the electronics [10, 11]. This spreading can be accounted for by using a probability function $P(E_i, E_j)$ [10, 11], which gives the probability that an α-particle which under ideal conditions would be recorded in channel i with energy E_i is now recorded in channel j with energy E_j. Evans [12] has shown that for a large number of collisions, $P(E_i, E_j)$ can be approximated by a Gaussian curve.

To obtain the concentration profile $c(x, t)$ there are two procedures which may be used. In the first procedure, an appropriate mathematical model is chosen to describe $c(x, t)$ and $P(E_i, E_j)$ is used to obtain a distorted spectrum as follows:

$$N_i^c = \sum_j N_j^0 P(E_i, E_j),$$

where N_j^0 is the calculated spectrum and N_i^c is the trial spectrum. This is commonly referred to as a convolution procedure [13] and the trial spectrum $[N_i^c]$ is fitted with the recorded spectrum $[N_i]$. In the second procedure, the undistorted spectrum and hence $c(x, t)$ are obtained directly from the recorded spectrum and the experimental spreading function. This is commonly referred to as the deconvolution procedure [13]. Thus the parameters involved in the diffusion model are inferred either by fitting the recorded spectra with the convoluted profiles or by fitting the deconvoluted spectra with undistorted profiles.

3. Self-diffusion phenomenology

A self-diffusion coefficient can be determined from the diffusion of a labelled isotope through a matrix of uniform chemical composition, except for the isotopic variation. Since our specimens are slabs with lengths and widths large compared to the depths of diffusion, the appropriate diffusion equation is

$$\frac{\partial C(x,t)}{\partial t} = D\frac{\partial^2 C(x,t)}{\partial x^2} \qquad (1)$$

where the x-direction is perpendicular to the slab surface. The initial condition is

$$C(x, 0) = C_I$$

where $C_I = 0.002$, the natural isotopic abundance of ^{18}O. The boundary conditions result from the fact that our samples are thick compared to the depth probed $[C(\infty, t) = C_\infty = C_I]$ and from the analysis of the gas for ^{18}O at various times during the diffusion exchange. The isotopic fraction C_g could be described by a power series:

$$C_g(t) = \sum_{n=0}^{r} C_n t^{n/2} \qquad (2)$$

where $r \simeq 2$ and where C_n are constants.

If only diffusion controls the kinetics,

$$C(x,t) - C_\infty = \sum_{n=0}^{r} (C_n t^{n/2} - C_\infty \delta_{n0}) 2^n \Gamma \times (1 + \tfrac{1}{2}n) i^n \times \mathrm{erfc}[x/2(Dt)^{1/2}] \qquad (3)$$

where Γ is the gamma function and $i^n\mathrm{erfc}(x)$ is the nth integral of the complementary error function.

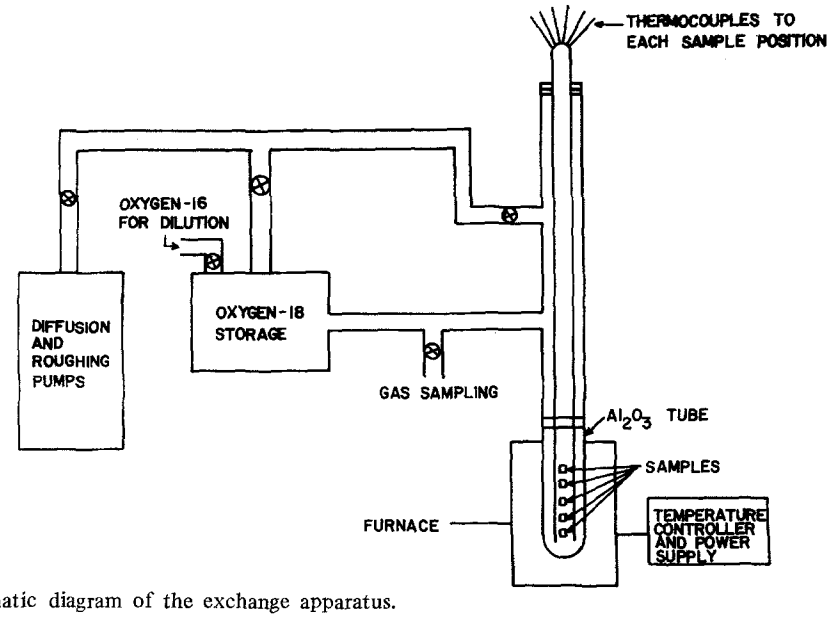

Figure 1 Schematic diagram of the exchange apparatus.

If the gas concentration is constant through the diffusion anneal, the above equation reduces to

$$C(x, t) - C_\infty = (C_0 - C_\infty) \operatorname{erfc} \frac{x}{2(Dt)^{1/2}}, \quad (4)$$

the familiar form of the error function solution.

4. Experimental details

4.1. Glass melting and sample preparation

Analytical grade reagents were used to prepare a batch corresponding to 200 g glass of composition $20\,K_2O$–$20\,SrO$–$60\,SiO_2$, numbers before the oxides indicating weight per cent. The batch was thoroughly mixed and melted in a 500 ml Pt–20% Rh crucible inside a globar electric resistance heating furnace at 1500° C for 1 h and then at 1400° C for 15 h. The melt was stirred a few times with a platinum stirrer to ensure homogeneity. The crucible was then placed in an annealing furnace at 650° C for 1 h and then very slowly cooled to room temperature. The glass block, removed from the crucible, was observed in polarized light to check for inclusions, bubbles and stresses and was found to be free of these.

10 mm square and 2.5 mm thick samples were cut from the block of glass with a diamond saw, the size being suitable for the sample holders of the annealing furnace and the Faraday cup. The samples were then ground and polished to 0.06 μm surface, unless otherwise specified.

4.2. Diffusion exchange

Fig. 1 shows a schematic diagram of the exchange apparatus. It is possible to place up to ten samples at a time in the five sample holder positions, and there are thermocouples next to each of these positions to record the temperature at which each sample is exchanged. The glasses were exchanged in ^{18}O-enriched atmosphere*; the ^{18}O was diluted with ^{16}O such that the partial pressure of oxygen is about 760 mm Hg. The ^{18}O-enriched gas was introduced into the system only after the temperature was stabilized and well-controlled in vacuum, and it was removed from the system only after each sample was cooled 100° C below the exchange temperature.

The variation of the ^{18}O concentration during the exchange was evaluated by taking frequent gas samples, eight to ten for each exchange anneal. The gas samples were then analysed by mass spectrometry at Sohio Research Laboratories in Cleveland.

The diffusion exchange was carried out for a short time, a medium time and a long time run corresponding to 76 860 sec (~ 22 h), 315 360 sec (~ $3\frac{1}{2}$ days) and 638 100 sec (~ $7\frac{1}{2}$ days), respectively.

4.3. Activation analysis

The activation analysis was carried out by bombarding the samples with protons with incident

*50% ^{18}O bought from Miles Laboratories Inc, Kankakee, Illinois 60901, USA.

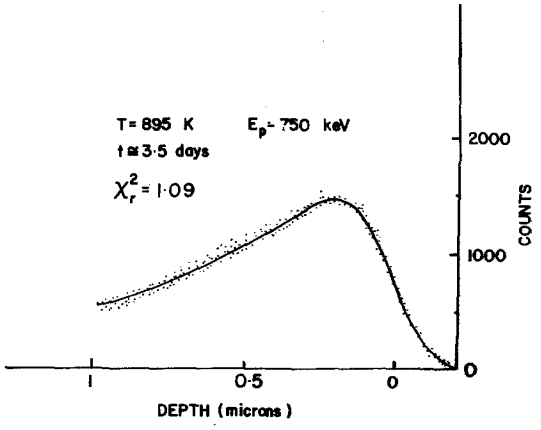

Figure 2 Experimental and calculated alpha spectra from the detector with the mylar.

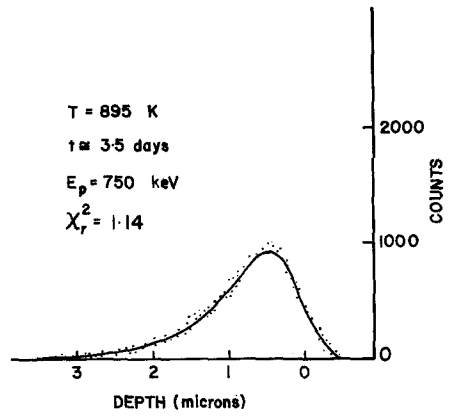

Figure 3 Experimental and calculated alpha spectra from the detector with the magnetic spectrometer.

energies of 750 or 800 keV, these being achieved on a 3 MeV Van de Graaff accelerator. The beam incident energy was known to better that ± 2 keV incident proton energy.

5. Data analysis

It was indicated in Section 2 that either a convolution or a deconvolution procedure can be used to obtain the parameters involved in the diffusion model. The choice of the procedure is dictated by the accuracy of the knowledge of the probability function $P(E_i, E_j)$. In the earlier stages of the use of the single spectrum technique [10] in our laboratory, the convolution procedure was used because the probability function was not accurately known. Also, the convoluted profiles are easy to derive to any accuracy and the computer computation times are reasonable. During the later stages of the development of the technique, Lindstrom and Heuer [11] used a Ta_2O_5 target (nominally 1009 Å thick) to generate the probability function and it was found to be Gaussian in shape. An accurate knowledge of the probability function is advantageous because the deconvolution of each spectrum has to be performed only once. Thus, the deconvolution procedure was used subsequently for all analysis.

To establish a relationship between the α-energy E_x and x, the stopping powders (dE/dx) for the glass and mylar must be known. Stopping powers of oxygen and silicon are listed in the compilation of Williamson *et al.* [14], but those of potassium and strontium had to be calculated by interpolation from two elements having lower atomic mass and two elements having higher atomic mass. The density of glass was determined in the laboratory to be 2.705 g cm^{-3}, and then the additive rule [12] for amorphous materials was used to calculate the stopping powers. Mylar stopping powers were similarly calculated by using $(C_{10}H_8O_4)_n$ as the general formula and 1.3875 g cm^{-3} as the density.

From the stopping powers and the α-energies as a function of x, spectra were generated and compared with the experimental spectra using a computer program. Unless otherwise specified, only Dt, where D is the self-diffusion coefficient and t is the exchange time, was varied to fit the generated spectra to the experimental spectra using a non-linear regression scheme [15] based on the χ^2 test, the minimum reduced χ_r^2 giving the best Dt values.

6. Results and discussion

Fig. 2 shows a typical experimental alpha spectrum from the mylar detector for a sample diffusion annealed for $3\frac{1}{2}$ days at 895 K. The incident porton energy was 750 keV. The figure also shows a solid line which is a computer fit generated with an erfc solution convoluted with the experimental probability function with a standard deviation of 60 keV. Only two parameters, the self diffusion coefficient D and time t, were used to obtain the generated spectrum. The excellent fit ($\chi_r^2 = 1.09$) shows that the diffusion profiles are indeed of the form of an erfc. This suggests that the kinetics are diffusion controlled. Fig. 3 shows a typical experimental alpha spectrum from the detector with the magnetic spectrometer for the same specimen. Once again an excellent fit ($\chi_r^2 = 1.14$) is obtained between the two spectra. When the incident proton energy was increased to 800 keV, excellent fits between the experimental and generated spectra were once again obtained and the D values

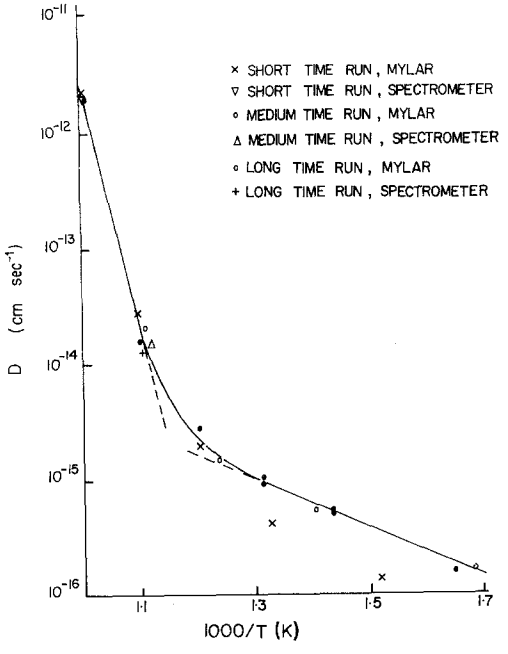

Figure 4 Log D versus $1/T$(K).

were the same within experimental error. This shows that the technique is consistent.

To show typical values, results for the long time run ($\sim 7\frac{1}{2}$ days) are listed in Table I. In the table the temperature refers to the temperature at which the samples were diffusion annealed, the surface refers to the surface preparation of the samples and the detectors MY and MS refer to the mylar and the magnetic spectrometer, respectively. Comparison of the D values of specimens with different surface preparations shows that the results of surface preparations of 0.06 and 9 μm are the same within experimental error; however, the one with an as-cut surface has a diffusion coefficient about an order of magnitude larger than the one with either the 9 or the 0.06 μm surface preparation. This shows the adequacy of the surface preparation.

The self-diffusion coefficients obtained for the three diffusion runs using the two detectors are plotted as logarithm of D against inverse of absolute temperature in Fig. 4. The figure shows two straight lines (the points being fitted by a least squares estimate) joined by a curve in the region of the glass transition. The short time run results above $1/T = 0.001\,25$ were not considered in the calculations of the best fits since they gave results that were consistently lower than the long and medium time runs. Above the glass transition temperature, T_g,

$$D = 7.6 \times 10^{+14} \exp(-119\,\text{kcal}/RT)\ \text{cm}^2\,\text{sec}^{-1}$$

and below T_g,

$$D = 1 \times 10^{-12} \exp(-10\,\text{kcal}/RT)\ \text{cm}^2\,\text{sec}^{-1}.$$

The value of T_g determined from thermal expansion experiment was around 600° C, in good agreement with the value corresponding to the intersection of the two straight lines in Fig. 4.

6.1. Accuracy and precision of the diffusion coefficients

As discussed elsewhere for ZnO [10], the most important uncertainty in determining $(Dt)_i$, determined for each channel i, comes from the stopping power estimates of the glass. A 20% error in the stopping powers of protons in the glass can cause a systematic 0.56 uncertainty in $\mathrm{d}(Dt)_i/(Dt)_i$. However, systematic errors do not affect activation energies and can be corrected later when better estimates of stopping powers are made available. Therefore, it is desirable to look into the random errors in the technique.

The sensitivity of the analysis is related to the

TABLE I Diffusion data for the long time run. Glass: 20 K_2O–20 SrO–60 SiO_2 (wt %); exchange time, 638 100 sec; $K = \infty$.

Temperature (K)	Surface (μm)	Detector	$Dt \times 10^8$ (cm^2)	D (cm^2 sec^{-1})	χ_r^2
900	0.06	MY	1.00	1.6×10^{-14}	1.09
900	9	MY	0.95	1.5×10^{-14}	1.32
900	0.06	MS	0.85	1.3×10^{-14}	1.11
900	9	MS	0.85	1.3×10^{-14}	1.14
832	0.06	MY	0.14	3.1×10^{-15}	1.08
760	0.06	MY	0.066	1.0×10^{-15}	1.29
760	9	MY	0.062	9.7×10^{-16}	1.24
760	As-cut	MY	1.00	1.6×10^{-14}	–
698	0.06	MY	0.037	5.8×10^{-16}	1.22
608	0.06	MY	0.010	1.6×10^{-16}	2.81

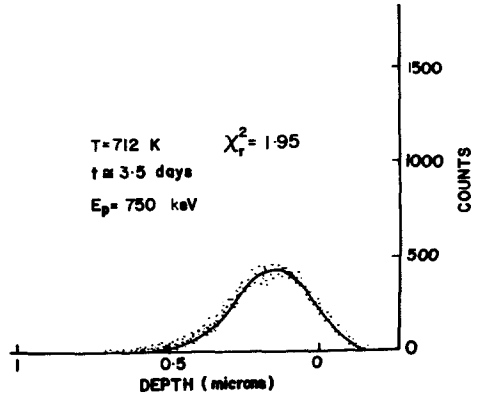

Figure 5 Experimental and calculated alpha spectra from the detector with the mylar illustrating low depths of diffusion.

uncertainty in determining the concentration of ^{18}O at the depth corresponding to the recorded energy, and the resolution is the uncertainty in determining the depth from which the recorded α-spectra in channel i has been emitted. The uncertainties of sensitivity and resolution are independent [10]. The simplest diffusion model has the gas concentration constant and the surface exhange coefficient $K = \infty$. Then from differentiation of Equation 4, squaring, and dropping the cross terms,

$$\left(\frac{d(Dt)_i}{(Dt)_i}\right)^2 = \left(\frac{G(\theta_i')}{C_0 - C_\infty}\right)^2 \left(\frac{\delta C_i^r}{C_i}\right)^2 + 4\left(\frac{\delta x_i^r}{x_i}\right)^2 \quad (5)$$

$(Dt)_i$, C_i (substituted for $C(x, t)$) and x_i are respectively the diffusion coefficient time product, concentration, and the depth associated with channel i. The superscript r indicates random nature of the error and

$$G(\theta_i) = \pi^{1/2} \exp(\theta_i^2)/\theta_i.$$

As defined above, δC_i^r and δx_i^r are associated with the sensitivity and the resolution of the analysis. Equation 5 shows that for small x_i, $\delta(Dt)_i$ is dominated by resolution of "near-surface" channels, and for large x_i the sensitivity becomes more important. The "near-surface" channels and the resolution become particularly important in the case of shallow diffusion depths. Then x_i is small and $\delta(Dt)_i^r$ is large. The low counts in each channel and the near-Gaussian shapes of the spectra make it difficult to distinguish between the effects of changes in Dt values and, for example, changes in K. Fig. 5 shows the alpha spectra, experimental and generated, for a specimen which was diffusion annealed at 712 K for $\sim 3\frac{1}{2}$ days. In this case $\chi_r^2 = 1.95$, indicative of a poor fit. These near-Gaussian spectra are in contrast to the results of Fig. 2 where the Dt values are large and both the shallow part of the spectrum called the "front-edge" and the deep part of the spectrum called the "tail" have to be fitted with the generated spectrum. This makes fitting independent of any parameter like K as demonstrated by the low χ_r^2 values obtained earlier.

The results of Fig. 4 show that for $1/T > 0.001\,25$, the diffusion coefficients obtained from the low-temperature short-time data were consistently low, possibly because of a low value of the surface exchange coefficient K, limiting the total exchange [16]. During the first stage of the analysis, only two parameters D and t were systematically varied and the χ_r^2 values obtained were no better than 1.95. However, when a lower K was systematically introduced, the fits improved considerably and χ_r^2 values of 1.35 were possible. This suggests that a contribution of K has to be considered to fit the low-temperature short-time data. The details of these results, are given elsewhere [17] and will be discussed in a later publication [18] where results at these and lower temperatures will be treated in detail and will reveal new features about K. As mentioned earlier, part of the discrepancy between the low-temperature short-time results and the results of longer times is due to the inability to obtain good fits because of the near-Gaussian spectra with low counts per channel.

The uncertainties in D evaluated from the uncertainties in diffusion time, δt, and the exchange temperature, δT, indicate that these uncertainties do not significantly affect the fractional precision of D [17].

6.2. Comparison with published work

6.2.1. Oxygen diffusion below T_g

The two distinct features of the results of this study below T_g are a small activation energy, 10 kcal mol^{-1}, and an extremely small pre-exponential factor, 1×10^{-12} cm^2 sec^{-1}. The values reported [19–26] for the activation energies for oxygen diffusion in glasses range from 11 to 75 kcal mol^{-1} and the pre-exponential factors range from 10^3 to 10^{-10} cm^2 sec^{-1}.

Kingery and Lecron [24] studied the oxygen diffusion in 12.8 CaO–15.5 Na_2O–71.7 SiO_2 (in this section, numbers before each oxide indicate mol%) and in 45.3 CaO–12.4 Al_2O_3–42.3 SiO_2 glasses and found that the activation energies were

66.5 and 59.0 kcal mol^{-1}, respectively, and the corresponding pre-exponential factors were 2.0×10^3 and 7.5×10^{-3} $cm^2 sec^{-1}$, respectively. Hagel and Mackenzie [25] determined the oxygen diffusion in 45.0 CaO–13.3 Al_2O_3–41.7 SiO_2 and in 42.2 CaO–15.7 Al_2O_3–42.1 B_2O_3 glasses and found that the activation energies were 57.7 and 35.4 kcal mol^{-1}, respectively, whereas the pre-exponential factors were 2.8×10^{-3} and 9.5×10^{-7} $cm^2 sec^{-1}$, respectively. Sucov [20] and Haul and Dumbgen [19] studied the oxygen diffusion in fused silica and found the activation energies of 71.0 and 56.0 kcal mol^{-1}, respectively, and the pre-expontial factors of 1.5×10^{-2} and 4.3×10^{-6} $cm^2 sec^{-1}$, respectively. In all cases, as the activation energy decreases, the pre-exponential factor decreases. All experiments involved an exchange reaction between the glass and oxygen gas of an isotopic ratio different from that of natural gas. Because these exchange experiments should be carried out over a large surface area of the glass investigated, the above experiments used glass powders, spheres and fibres. Because of phase boundary reactions, only if the exchange times are sufficiently long is the isotopic exchange rate determined by diffusion.

Williams [21] studied oxygen diffusion in fused silica, again by means of heterogeneous isotopic exchange for various diffusion times and he accounted for the surface exchange coefficient K. He determined the activation energy and the pre-exponential factor to be 29 kcal mol^{-1} and 2.0×10^{-9} $cm^2 sec^{-1}$, respectively. Schaeffer and Oel [26] studied oxygen diffusion in 33.0 PbO–8.7 K_2O–53.4 SiO_2 and 69.0 PbO–31.0 B_2O_3 glasses by pressing 50 to 100 μm layer of glass containing ^{18}O on bulk specimens, and determined the concentration profiles by subsequent annealing and serial sectioning. The corresponding activation energies were 12.0 and 11.0 kcal mol^{-1}, respectively, and the pre-exponential factors were 1×10^{-10} and 6×10^{-10} $cm^2 sec^{-1}$, respectively.

By studying the diffusion of oxygen in fused silica as a function of time, Williams [21] concluded that at high temperatures, for example 1250° C, the diffusion coefficients at either short or long times were nearly the same but at low temperatures, for example 950° C, the diffusion coefficients at short times were much lower compared to those determined at long times. This indicated that short exchange times would result in a larger temperature dependence of D giving larger activation energies and larger pre-exponential factors. The results of our short time run below T_g (Fig. 4), illustrate that if the data points of this run only are considered, the activation energy obtained is about twice as large compared to the 10 kcal mol^{-1} value determined from the medium- and long-time run results. The pre-exponential factor increases correspondingly, as expected from the discussion above. These observations are similar to the general trend of the results obtained by Williams [21] and these have been discussed in terms of K in Section 6.1.

Below T_g, Doremus [27, 28] and Meek [29] suggest that oxygen diffuses as molecules, that molecular oxygen also rapidly exchanges with the "lattice" oxygen and the solubility of oxygen in glass is approximately constant. The low values of activation energies obtained in our glass rule out the viscosity and exchange with the lattice oxygen as the rate controlling mechanisms [27] and suggest that the oxygen diffuses as molecules [27].

6.2.2. Oxygen diffusion above T_g

Above T_g, Ueda and Oishi [30] show that for a 44 CaO–14.9 Al_2O_3–41.1 SiO_2 glass, there is a large increase in the activation energy for oxygen diffusion compared to the value below the transition temperature. The activation energy for diffusion again becomes smaller in the molten region and the value is about the same as it is below T_g. Terai and Oishi [31] have studied the oxygen diffusion in a soda-lime silicate glass in the transition range and they observe that the diffusion coefficients, the activation energy and the pre-exponential factor increase rapidly with increasing temperature in this range. Fig. 4 shows the rapid increase of the activation energy, the increase being progressive as the temperature increases in the glass transition range, a behaviour similar to the results of Terai and Oishi [32]. This increase of the activation energy and the pre-exponential factor in the transition range is explained by the theory proposed by Adams and Gibbs [32]. According to their theory, the steep temperature dependence of the diffusion coefficient can be explained in terms of an excess structural activation energy required for migration of oxygen ions. This has been discussed in terms of a non-Arrhenius relation of the viscosity in the transition range by several authors [33–35].

As stated earlier, the fits of experimental and generated alpha spectra yield simple erfc solutions

for the oxygen concentration profiles and log D versus $1/T(K)$ above the transition range is a straight line. This rules out any chemical or internal reactions. This is in contrast to the diffusion studies of hydrogen [36, 37] which exhibits "abnormal" diffusion.

7. Conclusions

Oxygen self-diffusion studies carried out in a $20K_2O$–$20SrO$–$60SiO_2$ glass using a nuclear reaction, $^{18}O(p, \alpha)^{15}N$, yielded experimental alpha spectra which were fitted with computer-generated spectra to obtain oxygen concentration profiles which were simple erfc solutions both above and below T_g. It is suggested that oxygen diffuses as molecules below T_g in our glass. The rapid increase of the diffusion coefficients above T_g is explained in terms of an excess structural activation energy needed for migration of oxygen ions.

Acknowledgements

The financial support of Goddard Space Flight Center and NSF are gratefully acknowledged. We wish to thank Dr Lindstrom and Dr Heuer for their help at various stages of this work. The assistance of L. Major and R. Bernard is acknowledged.

References

1. A. K. VARSHNEYA and A. R. COOPER, *J. Amer. Ceram. Soc.* **51** (1968) 103.
2. *Idem, ibid* **55** (1972) 220.
3. *Idem, ibid* **55** (1972) 312.
4. *Idem, ibid* **55** (1972) 418.
5. G. AMSEL, J. P. NADAI, E. D'ARTEMARE, D. DAVID, E. GIRARD and J. MOULIN, *Nucl. Instr. Methods* **92** (1971) 481.
6. G. AMSEL, G. BERANGER, B. DEGOLAS and P. LACOMBE, *J. Appl. Phys.* **39** (1968) 2246.
7. G. AMSEL and D. SAMUEL, *Anal. Chem.* **39** (1967) 1639.
8. A. CHOUDHARY, D. W. PALMER, G. AMSEL, H. CURIEN and P. BARUCH, *Solid State Commun.* **3** (1965) 119.
9. D. W. PALMER, *Nucl. Instr. Methods* **38** (1965) 187.
10. R. ROBIN, A. R. COOPER and A. H. HEUER, *J. Appl. Phys.* **44** (1973) 3770.
11. W. W. LINDSTROM and A. H. HEUER, *Nucl. Instr. Methods* **116** (1974) 145.
12. R. D. EVANS, "The Atomic Nucleus" (McGraw-Hill, New York, 1965).
13. W. KAPLAN, "Operational Methods for Linear Systems" (Addison Wesley, London, 1962).
14. C. F. WILLIAMSON, J. P. BOUJOT and J. PICARD, Centre d'Etudes Nucleaires de Saclay, Report No. CEA-R-3042 (1966).
15. P. R. BEVINGTON, "Data Reduction and Error Analysis for the Physical Sciences" (McGraw-Hill, New York, 1969).
16. J. CRANK, "Mathematics of Diffusion" (Oxford, London, 1956) p. 34.
17. B. S. RAWAL, M.S. Thesis, Case Western Reserve University, Cleveland, Ohio (1974).
18. B. S. RAWAL and A. R. COOPER, *J. Non-Cryst. Solids* (to be submitted).
19. R. HAUL and G. DUMBGEN, *Z. Electrochem.* **66** (1962) 636.
20. E. W. SUCOV, *J. Amer. Ceram. Soc.* **46** (1963) 14.
21. E. L. WILLIAMS, *ibid* **48** (1965) 190.
22. F. J. NORTON, *Nature* **191** (1961) 701.
23. R. M. BARRER, "Diffusion in and Through Solids" (Cambridge University Press, New York, 1952) p. 126.
24. W. D. KINGERY and J. A. LECRON, *Phys. Chem. Glasses* **1** (1960) 87.
25. W. C. HAGEL and J. D. MACKENZIE, *ibid* **5** (1964) 113.
26. H. A. SCHAEFFER and H. J. OEL, *Glastech. Ber.* **42** (1969) 493.
27. R. H. DOREMUS, "Glass Science" (Wiley, New York, 1973) Ch. 8.
28. *Idem, J. Non-Cryst. Solids* **25** (1977) 261.
29. R. L. MEEK, *J. Amer. Ceram. Soc.* **56** (1973) 341.
30. H. UEDA and Y. OISHI, Semi Annual Report of the Asahi Glass Foundation for the Contribution to Industrial Technology **16** (1970) 201.
31. R. TERAI and Y. OISHI, *Glastech. Ber.* **50** (1977) 68.
32. G. ADAMS and J. H. GIBBS, *J. Chem. Phys.* **43** (1965) 139.
33. M. L. WILLIAMS, R. F. LANDEL and J. D. FERRY, *J. Amer. Chem. Soc.* **77** (1965) 3701.
34. M. H. COHEN and D. TURNBULL, *J. Chem. Phys.* **31** (1959) 1164.
35. P. B. MACEDO and T. A. LITOVITZ, *ibid* **42** (1965) 245.
36. R. W. LEE, *ibid* **38** (1963) 448.
37. R. W. LEE, R. C. FRANK and D. E. SWETS, *ibid* **36** (1962) 1062.

Received 5 September and accepted 12 October 1978.